

to Dr. H. P. Broida for providing the plasma afterglow sources and excellent laboratory facilities. Informative discussions with Dr. H. P. Broida,

Dr. M. Butler, and Dr. Stanton Peale were most useful in formulating the model to explain the population distribution.

*Work supported in part by the Advanced Research Projects Agency and the U.S. Office of Naval Research.

¹E. Hinnov and J. G. Hirschberg, *Phys. Rev.* **125**, 795 (1962).

²J. A. Thornton, Litton Publication No. 11-68-190, 1968 (unpublished).

³C. B. Collins and W. W. Robertson, *J. Chem. Phys.* **40**, 2202 (1964).

⁴E. E. Ferguson, F. C. Fehsenfeld, and A. L. Schmeltekopf, in *Advances in Atomic and Molecular Physics* (Academic, New York, 1969).

⁵A. F. Kuckes, R. W. Motley, E. Hinnov, and J. G. Hirschberg, *Phys. Rev. Letters* **6**, 337 (1961).

⁶N. D'Angelo, *Phys. Rev.* **121**, 505 (1961).

⁷J. L. Dunn, Ph.D. thesis (University of California at Santa Barbara, 1966) (unpublished).

⁸E. U. Condon and G. H. Shortley, *The Theory of Atomic Spectra* (Cambridge U. P., London, 1963).

⁹W. C. Martin, *J. Res. Natl. Bur. Std.* **64A**, 19 (1960).

¹⁰L. Goldberg, *Astrophys. J.* **90**, 414 (1939).

¹¹W. L. Wiese, M. W. Smith, and B. M. Glennon, *Atomic Transition Probabilities*, Vol. I (U. S. Department of Commerce, Washington, D. C., 1966), NSRDS-NBS 4.

¹²C. B. Childs, *Appl. Opt.* **1**, 711 (1962).

¹³D. R. Bates and A. Dalgarno, in *Atomic and Molecular Processes*, edited by D. R. Bates (Academic, New York, 1962), Chap. 7.

¹⁴Lyman Spitzger, Jr., *Physics of Fully Ionized Gases*

(Wiley, New York, 1962), Chap. 5; *Monthly Notices Roy. Astron. Soc. (London)* **100**, 396 (1940).

¹⁵Donald W. Marquardt, *J. Indian Soc. Appl. Math.* **11**, No. 2, 431 (1963).

¹⁶This means that a linear fit to the data for small n would yield a value for T_2 which is higher than that obtained by using Eq. (10). For the present experiment, it was about 15% higher.

¹⁷S. R. Byron, R. C. Stabler, and P. I. Bartz, *Phys. Rev. Letters* **8**, 376 (1962).

¹⁸The possibility that the high-temperature electrons originated from the cathode or discharge region was eliminated because it was found that the temperature of these electrons was independent of the potential applied to the cathode between 300 and 1500 V.

¹⁹There most likely exist in the afterglow small monoenergetic groups of electrons at 24.6 and, perhaps, 20 eV. The former group originates from recombination and the latter from collisions with metastables. These groups will contribute some energy to the high-temperature electrons.

²⁰B. S. Tanenbaum, *Plasma Physics* (McGraw-Hill, New York, 1967).

²¹C. B. Collins and W. W. Robertson, *J. Chem. Phys.* **40**, 2208 (1964).

²²M. S. Manalis, Ph.D. thesis (University of California at Santa Barbara, 1970) (unpublished).

²³Kerson Huang, *Statistical Mechanics* (Wiley, New York, 1963).

Observation of Quantum Phase Fluctuations in Infrared Gas Lasers*

K. R. Manes[†] and A. E. Siegman

Department of Electrical Engineering, Stanford University, Stanford, California 94305

(Received 18 September 1970)

By heterodyning together the outputs from two stable He-Ne 3.39- μ lasers, we have measured the power spectrum of the laser field over a wide range of output powers. By combining this high-gain laser transition with a very lossy laser cavity, the quantum phase noise contribution to the laser linewidth could be made dominant at low output powers. The laser spectrum was then found to be nearly Lorentzian with a bandwidth inversely proportional to output power, in good agreement with a modified form of the Schawlow-Townes laser linewidth formula. Weak quantum-noise-excited sidebands were also observed in the beat spectrum of a He-Xe 3.508- μ laser. These were identified with a resonance in the He-Xe laser amplitude-fluctuation spectrum.

I. INTRODUCTION

Even in a high-quality stable single-frequency laser oscillator, the instantaneous laser phase and amplitude will retain some noise fluctuations. These are usually caused in practical situations by

various external disturbances sometimes called "technical noise,"¹ referring to microphonics, structural vibrations, plasma oscillations, and other environmental disturbances. In addition, as a fundamental or ultimate limiting source of noise there are quantum amplitude and quantum phase

fluctuations that arise from the basic process of atomic spontaneous emission in the laser medium. The technical- and the quantum-noise sources can be experimentally distinguished, since the technical-noise sources usually result in a Gaussian laser spectrum, while the quantum-noise sources give a Lorentzian spectrum to the laser. The short-term Gaussian spectrum contributors together with long-term thermal and pressure drifts can always be reduced, at least in principle. Quantum noise, however, provides a limit beyond which no additional quieting of the surroundings can reduce the fluctuations of the laser or narrow its spectrum. Quantum-caused amplitude fluctuations in lasers have previously been measured in extensive detail with remarkable agreement between experiment and theory.²⁻⁶ Quantum phase fluctuations have also been observed to some extent previously,⁷⁻¹⁰ but with some limitations on the scope of the experimental results. The purpose of this work was to measure in detail the quantum phase fluctuations in a gas laser, and to compare the measurements with theory.

Theoretical discussions to date have arrived at the following prediction for the quantum-noise contribution to the above-threshold oscillation linewidth of a homogeneous laser tuned to atomic line center:

$$\Delta f_a = \frac{\pi h f (\Delta f_c)^2}{P_{\text{out}}} \frac{N_2}{N_2 - (g_2/g_1) N_1}, \quad (1)$$

where Δf_a is the full Lorentzian linewidth, N_2 and N_1 are the populations of the upper and lower laser level, P_{out} is the laser output power, f is the oscillation frequency, and Δf_c is the "cold cavity" bandwidth.¹¹ Because Eq. (1) multiplied by 2 yields the linewidth originally predicted by Schawlow and Townes, this expression is generally known as the Schawlow-Townes formula.¹²

Early interferometric measurements put rather broad upper bounds on the laser linewidth, and established that a laser cannot be described merely as a linear amplifier of narrow-band Gaussian noise.¹³ Some more detailed phase-fluctuation measurements were made earlier in this laboratory by heterodyning the outputs from two extremely stable 6328-Å He-Ne lasers.^{7, 8, 14} In the best of these experiments, the technical noise gave the lasers a predominantly Gaussian line shape with a bandwidth of approximately 3.5 kHz, compared to a Lorentzian quantum linewidth contribution of, at most, a few hundred Hz. Because of their differing statistical properties, the Lorentzian quantum fluctuations could still be separated from the Gaussian background and measured under these conditions, but the laser spectrum was still predominantly Gaussian when viewed with a spectrum analyzer in all cases. The Lorentzian line shape

caused by quantum phase noise was later directly observed by Hinkley and Freed in a $\text{Pb}_{0.88}\text{Sn}_{0.12}$ Te diode laser.¹⁰ The measurements on this laser, however, covered only a very small power range.

This paper presents first the results of a simplified quantum theory of the laser oscillator.¹⁵ The predictions of this theory are then compared to experimental observations on 3.39- μ He-Ne and 3.508- μ He-Xe lasers above threshold over a wide range of output power.

II. THEORETICAL RESULTS

Using a model proposed by Lax,¹¹ together with a density matrix technique,^{16, 17} one of us has derived an expression for the power spectral density of the E field of a single-mode laser oscillator above threshold.¹⁵ The theoretical prediction for the full bandwidth at half-maximum of the laser spectrum Δf_a depends on the statistical properties assumed for the Langevin spontaneous-emission noise sources. If δ -correlated (white) Langevin noise sources are assumed,^{11, 18-23} we recover the Schawlow-Townes formula of Eq. (1) in the form

$$\Delta f_a = \frac{\pi h f (\Delta f_c)^2}{P_{\text{out}}} \left(\frac{N_2^e}{\Delta N_0} + n^e \right), \quad (2)$$

where N_2^e is the upper-level population with the pump on, ΔN_0 is the population difference above threshold, and $n^e = (e^{hf_c/kT} - 1)^{-1}$ is the thermal-equilibrium blackbody photon number. For most lasers this last factor is negligible.

For an inhomogeneously broadened laser gain medium, the Schawlow-Townes formula may be given the modified form¹⁵

$$\Delta f_a = \frac{\pi h f (\Delta f_c)^2}{P_{\text{out}}} \left(\beta \frac{N_2^e}{\Delta N_0} + n^e \right). \quad (3)$$

If exponentially correlated (band-limited) Langevin spontaneous-emission noise sources are assumed, with correlation times equal to the atomic dephasing time T_2 due to soft collisions, then¹⁵

$$\beta = 1 + \frac{8 \ln 2}{(\Delta \omega_G T_2)^2} \left(\frac{1}{z} - 1 \right), \quad (4)$$

where $\Delta \omega_G$ is the Doppler-broadened linewidth of the laser transition, and the function z is related to the plasma dispersion function Z by

$$z \left[\left(\frac{1}{T_2} \right)^2, \Delta \omega_G \right] \equiv -i \frac{(4 \ln 2)^{1/2}}{\Delta \omega_G T_2} Z \left[i \frac{(4 \ln 2)^{1/2}}{\Delta \omega_G T_2} \right]. \quad (5)$$

This formula goes to 1 in the homogeneous case $\Delta \omega_G \rightarrow 0$, and to zero in the inhomogeneous limit. As a result, the factor β lies between 1 and 2, with $\beta \rightarrow 2$ corresponding to the homogeneous limit and $\beta \rightarrow 1$ to the inhomogeneous limit. For our He-Ne 3.39- μ lasers, $\beta \approx 1.5$.

Lax has observed that for a homogeneous medium, Δf_q should increase off the atomic line center according to¹¹

$$\Delta f_q(\omega_c) = \Delta f_q(\Omega_0) \left[1 + \left(\frac{\omega_c - \Omega_0}{1/2T_c + 1/T_2} \right)^2 \right], \quad (6)$$

where Ω_0 is atomic line center and ω_c is the cavity frequency. This occurs in essence because the frequency-pulling effect of the atomic transition couples a portion of the quantum amplitude fluctuations into the phase equation, thus increasing Δf_q . Presumably there will be a similar increase in Δf_q off line center in the inhomogeneous case.

III. EXPERIMENTS WITH He-Ne 3.39- μ LASER

The quantum contributions to laser spectral width can be enhanced relative to the technical and environmental contributions by using laser transitions with a high gain per unit length together with a low-Q laser cavity. Therefore, our measurements were carried out using two particularly high-gain gas laser transitions, primarily the He-Ne 3.39- μ transition and to a lesser extent the He-Xe 3.508- μ transition.

A. Experimental Arrangements

Direct observations of the laser spectrum were accomplished by heterodyning together the beams from two highly stable He-Ne 3.39- μ lasers. Figure 1 shows the essential features of the measurement apparatus. Both laser cavities consisted of a 100% reflecting 300-cm-radius mirror plus a flat variable-reflectivity output mirror, and a

Brewster-window plasma tube. Plasma tubes and mirror mounts were bolted firmly to polished Invar slabs 1 \times 5 \times 18 in. in such a way that the invar alone determined the 30-cm mirror spacing. All intracavity air paths were sealed. One of the lasers, called the signal laser, had a low-reflecting output mirror and thus a particularly low-Q cavity. It used a cold-cathode plasma tube with a bore diameter of 2.75 mm filled with 10% Ne²⁰ and 90% He⁴ to a total pressure of 2.4 Torr. The other or local-oscillator laser used a standard Spectra-Physics model No. 130 plasma tube (bore diameter equal to 2.5 mm) and an output mirror with 70% reflectivity, yielding about 700 μ W on line center. Both lasers operated in the TEM₀₀ mode.

The two lasers were positioned on a stable table consisting of a 6000-lb granite slab resting on a 6000-lb base of bricks in alternate layers with rubber rug pads. The entire assembly floated on 18 small rubber inner tubes in an underground vault.¹⁴ The vault temperature stayed at (16 ± 0.2) °C for the duration of the experiment. All power supplies, electronics, and measuring equipment were located in a separate control room connected to the lasers by shielded cabling. Particular care was taken to ensure that the plasma-tube power was well regulated and filtered.

The laser beat spectrum itself was the most sensitive measure of any disturbance. For example, in spite of all attempts at acoustic shielding, the fundamental frequency of the engine noise of passing automobiles was clearly visible in the laser beat spectra. For this reason, all data was

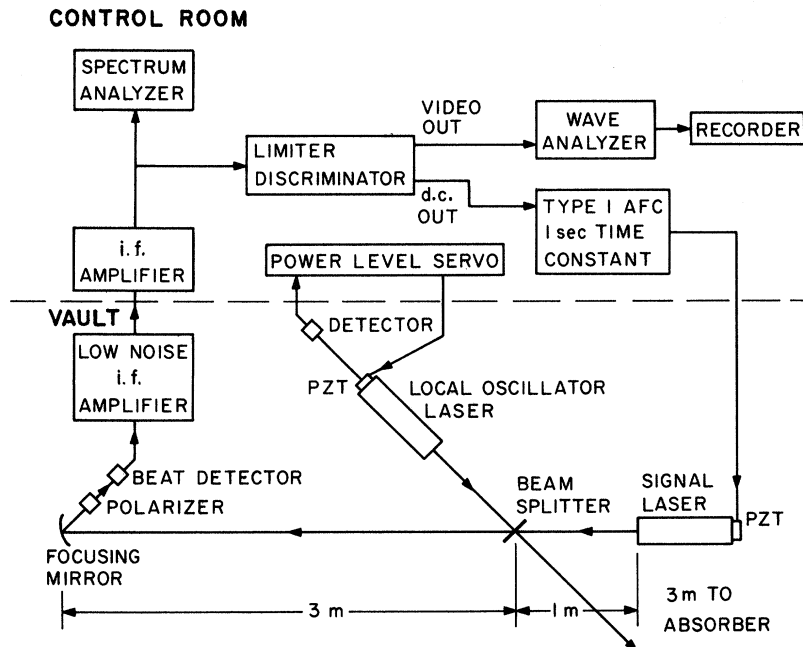


FIG. 1. Experimental setup for studying the spectrum of the heterodyne beat note between two stable He-Ne 3.39- μ lasers.

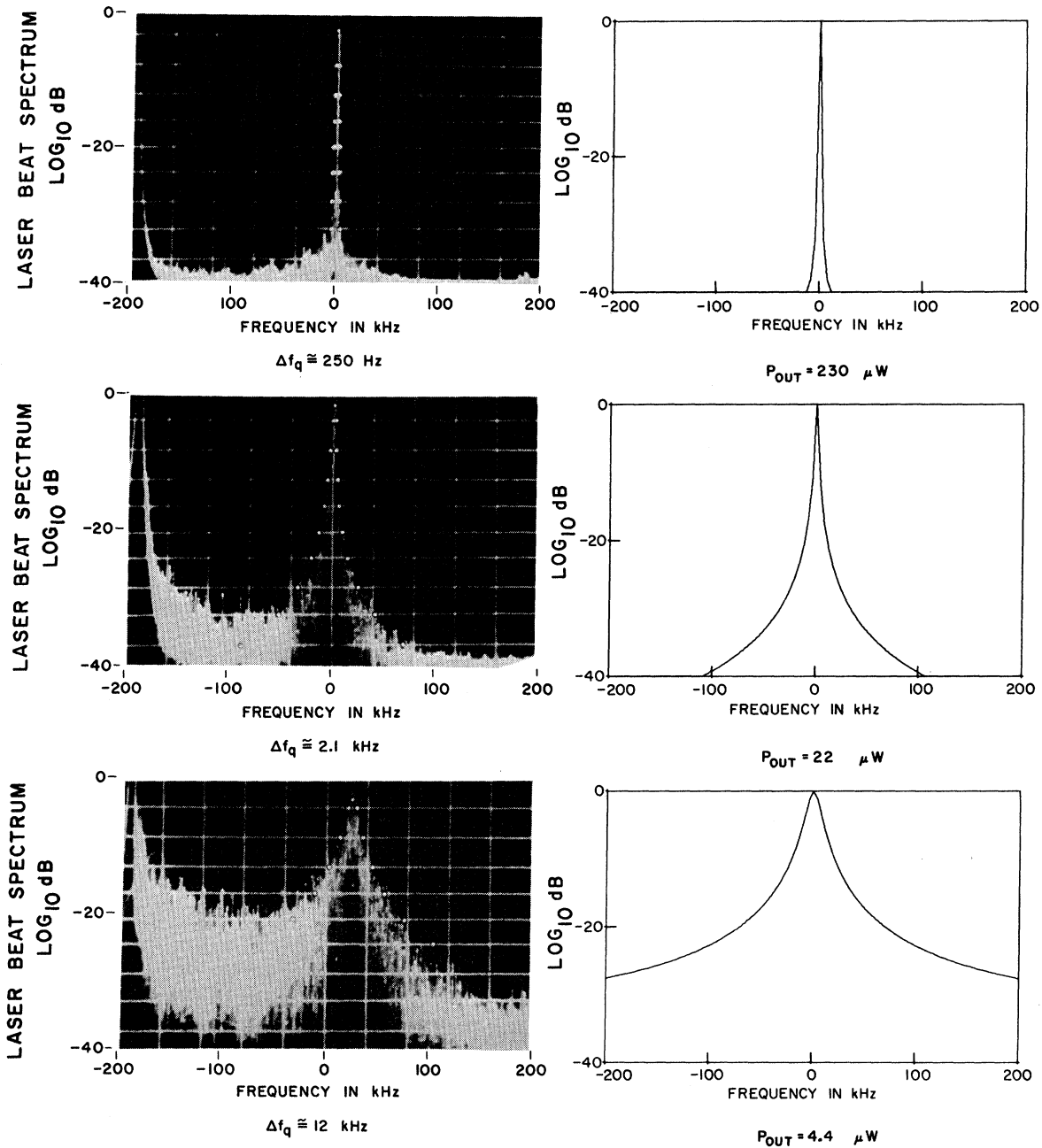


FIG. 2. Power spectrum (on log scale) on the 190-kHz beat between two He-Ne 3.39- μ lasers at three different output power levels of the signal laser, compared with computer-calculated curves. Laser output mirror reflectivity $\approx 3.5\%$, laser tuned to atomic line center.

taken at night. The low Q of the signal-laser cavity also made it particularly susceptible to backscatter coupling from the beam splitter and the detector. The radiation scattered back from these elements was minimized by (a) maximizing the distances to the elements, (b) using a high-quality beam splitter consisting of a two-layer dielectric coating on a thin quartz flat, and (c) rotating the linear polariza-

tion of the signal and local-oscillator beams by 90° until both beams reached a 45° polarizer located just before the detector.

The lasers were allowed to equilibrate for approximately 10 h with the vault sealed before a data run. Piezoceramic tuning stacks allowed the frequencies of both laser cavities to be tuned at ~ 1 MHz/V. Different beat frequencies between

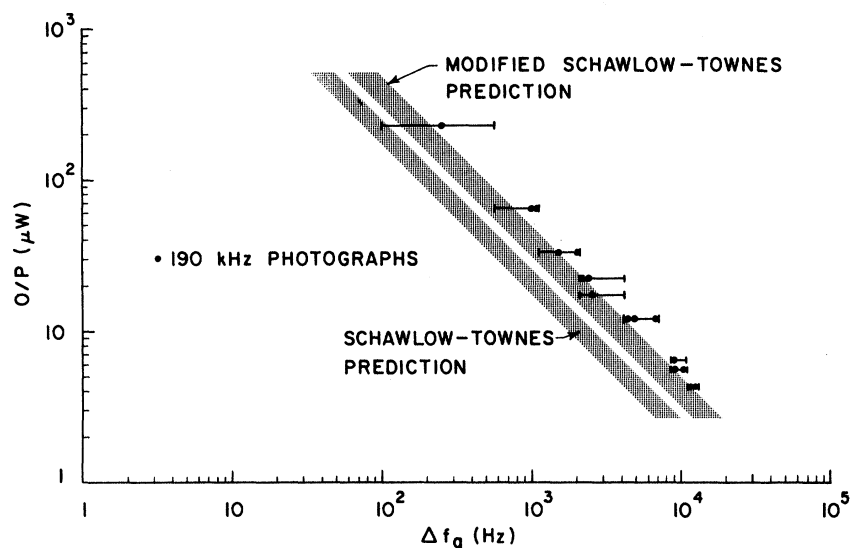


FIG. 3. Data from a series of photographs such as Fig. 2, plotted as signal-laser output power in μW vs Lorentzian quantum-noise linewidth of the laser in Hz.

lasers were used in different experiments, depending on the particular detector, amplifiers, and frequency discriminator employed. In each experiment the dc-coupled output from a beat-frequency discriminator provided the error signal for a simple automatic-frequency-control (AFC) circuit with a time constant of ~ 1 sec. Both lasers could generally be relied upon to stay within the 24-MHz-wide locking range of the AFC system for several hours.

To make a series of measurements, the signal laser was tuned to approximate line center and the AFC loop closed. With the beat locked and steady, the pump power to the signal laser was varied in small steps, allowing the system to equilibrate a few minutes each time. The beat spectrum was displayed on a spectrum analyzer and photographed; the video output spectrum of the frequency discriminator was recorded using a wave analyzer; and the beat power level was recorded. In order to avoid interaction between measuring devices, only one such device at a time was connected to the beat output. For each data run the detector sensitivity was calibrated with an Eppley thermopile, and the lasers were checked to ensure single-frequency operation.

In initial experiments the laser-threshold plasma current, even with an uncoated quartz output mirror (reflectivity $\sim 4\%$), was only ~ 1.8 mA, which was dangerously near the minimum current required to sustain the plasma discharge in this tube and therefore was in the region of plasma relaxation oscillations. Therefore, a number of permanent magnets were fixed to the outer wall of the plasma tube so as to somewhat reduce the laser gain at 3.39μ without noticeably altering the output power versus frequency line shape. The

laser-threshold current using an uncoated output mirror was shifted up in this way to ~ 5.5 mA, while the threshold for a 40% reflecting output mirror was moved up to ~ 2 mA.

B. Experimental Results

Two output mirror reflectivities on the signal laser, and a variety of frequency settings within the inhomogeneously broadened atomic line, were studied using several different beat frequencies. Each set of data represents a more or less independent check of the theory. Photographs of the laser beat spectra are compared in each case to computer-generated plots of the spectra predicted by the analysis.

1. Output Mirror Reflectivity $\approx 3.5\%$ on Atomic Line Center

The beat frequency in this case was 190 kHz, with a Hewlett-Packard 5210A frequency meter as the discriminator. The beat spectrum was displayed by a Singer Metrics model No. SPA-3 spectrum analyzer on the \log_{10} setting. The detector was a modified Texas Instruments InSb photoconductor cooled to 77°K . Representative photographs of the spectra are reproduced in Fig. 2, and a plot of Δf_q versus output power, using measurements from all photographs taken, appears in Fig. 3. The linewidth Δf_q was obtained by measuring the full bandwidth of the photographed spectrum at -20 dB and making use of the relation $\Delta f(-20 \text{ dB}) \approx 10\Delta f_q$, which is valid for Lorentzian spectra. The error limits were determined by overlaying the photographs with a transparency on which nine Lorentzian curves were drawn and estimating between which two curves the photographic spectrum lay.

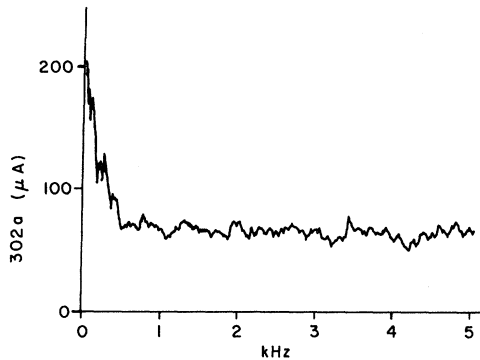


FIG. 4. Power spectral density, as recorded by a Hewlett-Packard 302A wave analyzer, of the video output of a frequency discriminator whose input is the 4.5-MHz beat between the two He-Ne 3.39- μ lasers. The spectrum is white above 1 kHz. Laser output mirror reflectivity $\approx 3.5\%$, laser tuned to atomic line center.

Measurements were also made on the same laser system using a 4.5-MHz beat frequency and an integrated-circuit limiter discriminator.¹⁸ The detector was a biased InAs photodiode (Philco L4530) at room temperature. In this case the power spectral density of the discriminator video output $S_d(\omega)$ was measured with an Hewlett-Packard 302A wave analyzer, as illustrated in Fig. 4. These measured discriminator output spectra showed $1/f^2$ dependence up to ~ 500 Hz, which indicates that the laser spectrum had a technical-noise-induced Gaussian bandwidth of 3–5 kHz.¹⁴ Above 500 Hz, however, the discriminator output spectrum was white up to 50 kHz, the limit of our apparatus. The white portion of $S_d(\omega)$ measures the contribution of the Lorentzian beat-spectrum characteristic of quantum phase noise.

The value of $S_d(\omega)$ in the flat portion is related to the full quantum-noise bandwidth Δf_q by

$$S_d(\omega) \approx K_d^2 \Delta f_q / 2\pi, \quad (7)$$

where K_d is the discriminator constant in V/Hz.

The resulting data for Δf_q versus laser output power from these measurements are plotted in Fig. 5.

Still another set of data was taken at a beat frequency of 30 MHz using an RHG model No. DT3006 discriminator and the same Philco L4530 detector. The measurements in this case were also made by measuring the discriminator video output spectrum $S_d(\omega)$, but this time we used only a single arbitrarily chosen frequency (30 kHz) well out into the white portion of the $S_d(\omega)$ spectrum. In taking this data, the wave analyzer was set at 30 kHz, and the wave-analyzer output plotted on an x - y recorder versus laser pump current. A separate measurement of laser output power versus laser pump current was taken immediately afterwards. The data from these measurements have also been plotted in Fig. 5.

2. Output Mirror Reflectivity $\approx 3.5\%$, Tuned to Edge of Atomic Line

In order to test for the expected increase in Δf_q off line center, measurements were taken using a 30-MHz beat frequency with the signal laser detuned ~ 220 MHz off the atomic line center. The beat spectrum in this case was displayed directly on a Polarad model No. 2992A spectrum analyzer and photographed. By means of a 30-MHz crystal oscillator and mixer the spectrum was also heterodyned down to 455 kHz, displayed on the Singer spectrum analyzer and photographed. Simultaneously, the quantum linewidth Δf_q was measured

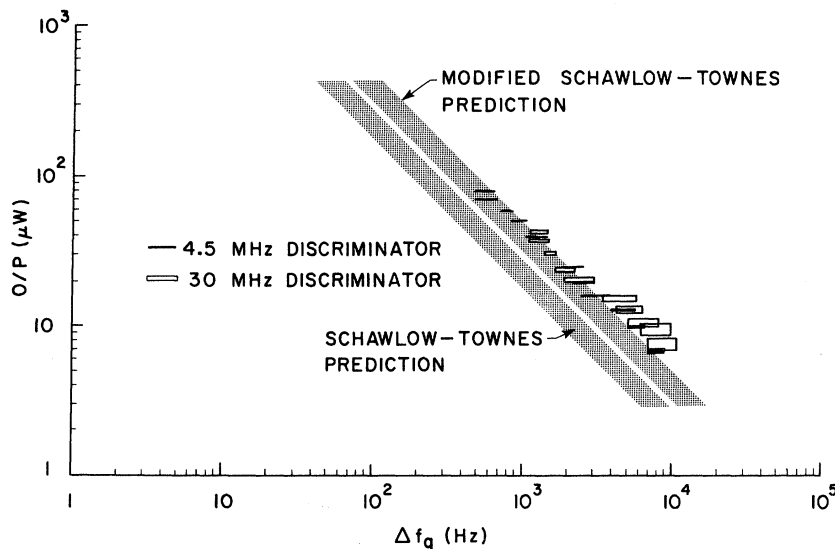


FIG. 5. Data from 4.5-MHz frequency discriminator runs such as Fig. 4, and from similar runs using a frequency discriminator at 30 MHz, plotted as output power vs quantum-noise linewidth.

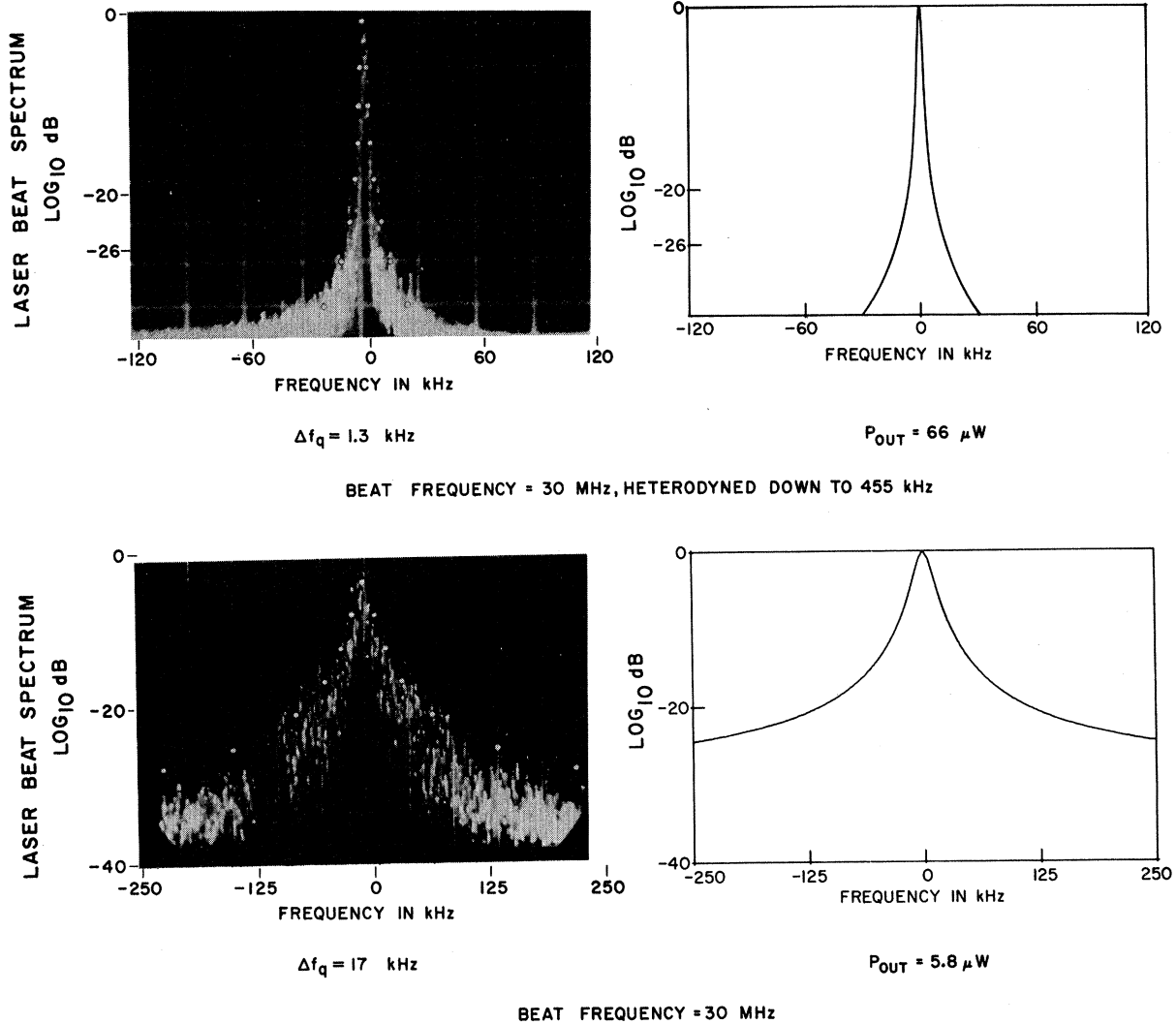


FIG. 6. Power spectrum of the 30-MHz beat between two He-Ne 3.39- μ lasers, on log scale, and corresponding theoretical curves, with the lasers tuned off line center. Output mirror reflectivity $\approx 3.5\%$; signal laser tuned ~ 220 MHz off line center.

using the discriminator method described above. Representative photographs of the spectra appear in Fig. 6, and the measured linewidth versus output power is plotted in Fig. 7. The homogeneous theory predicts a factor of 1.84 increase in linewidth for this amount of detuning off line center, in agreement with the increased linewidth experimentally observed.

3. Output Mirror Reflectivity $\approx 37.5\%$, near Atomic Line Center

With this higher output mirror reflectivity, the laser oscillation-threshold current with the cavity tuned exactly to line center (~ 1.8 mA) was so low that plasma relaxation oscillations were encountered. Therefore, the signal laser was tuned

~ 100 MHz off line center to increase the threshold current. Measurements were made using a 30-MHz beat frequency and the same apparatus as described above. The basic data, in the form of wave-analyzer output level versus laser plasma-tube current or laser power output, is plotted in Fig. 8. These results expressed as laser linewidth versus laser power output have also been included in Fig. 7. Again, the measured data lie very close to the homogeneous off-line-center correction.

IV. EXPERIMENTS WITH He-Xe 3.508- μ LASER

A. Experimental Arrangements

The $5d[3\frac{1}{2}]_3^0 - 6p[2\frac{1}{2}]_2$ transition in xenon (Racah

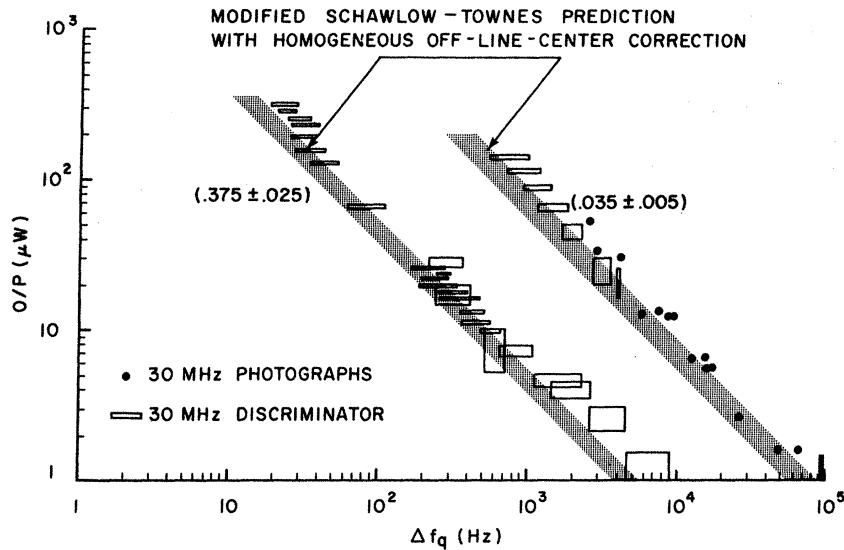


FIG. 7. Data from power spectral photographs, such as Fig. 6, and also from frequency discriminator runs, such as Fig. 8, plotted as laser output power vs quantum-noise linewidth. Output mirror reflectivities are 37.5 and 3.5%; laser tuned ~ 100 and ~ 200 MHz off line center.

notation) employed in the He-Xe laser provides one of the highest-gain laser systems known.²⁴ With 3-mm-bore-diam natural-abundance Xe plasma tubes, we routinely achieved gains of ~ 120 dB/m. Because of its high gain, the He-Xe laser may be operated with an extremely low- Q laser cavity. It is, therefore, an attractive candidate

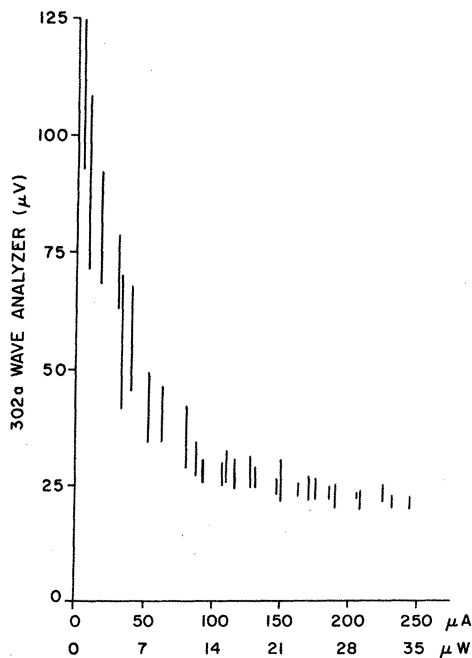


FIG. 8. Wave-analyzer output at 30 kHz (in the flat portion of Fig. 4) vs laser current and laser output power. He-Ne 3.39- μ lasers; 30-MHz beat; output mirror reflectivity $\approx 37.5\%$; tuned ~ 100 MHz off line center. These data are also plotted in Fig. 7.

for quantum-noise experimentation. The rf excitation was chosen for our experiments because it is believed to produce a generally quieter plasma.²⁵ One major experimental difficulty is that He-Xe lasers often exhibit lifetimes of only a few hours because of too rapid xenon cleanup. To overcome this cleanup problem, our lasers were provided with sidearms and heavily overfilled with Xe. The sidearms were inserted into special temperature-control units held at $\sim 90^\circ$ K. The temperature-control units were cooled by liquid-nitrogen baths at 77° K. The differential resistivity of two germanium diodes, one in the liquid-nitrogen bath and one attached to the laser tube sidearm, provided an error signal for a servo-system which maintained the sidearm temperature fixed at $(87.5 \pm 0.1)^\circ$ K. At this temperature most of the xenon in the plasma tube crystallizes on the walls of the sidearm, leaving a vapor pressure of ~ 19 to ~ 22 mTorr of xenon, together with ~ 2 Torr of He⁴, in the laser tube. These pressures are near optimum for lasing.

Two such lasers were constructed and a two-

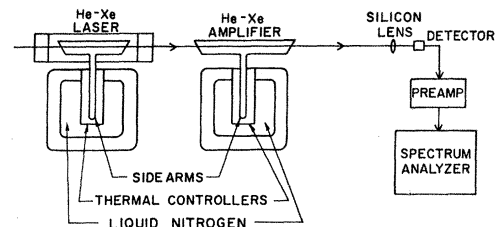


FIG. 9. Schematic of the two-transverse-mode He-Xe 3.5- μ laser oscillator, followed by a He-Xe laser amplifier and detector system.

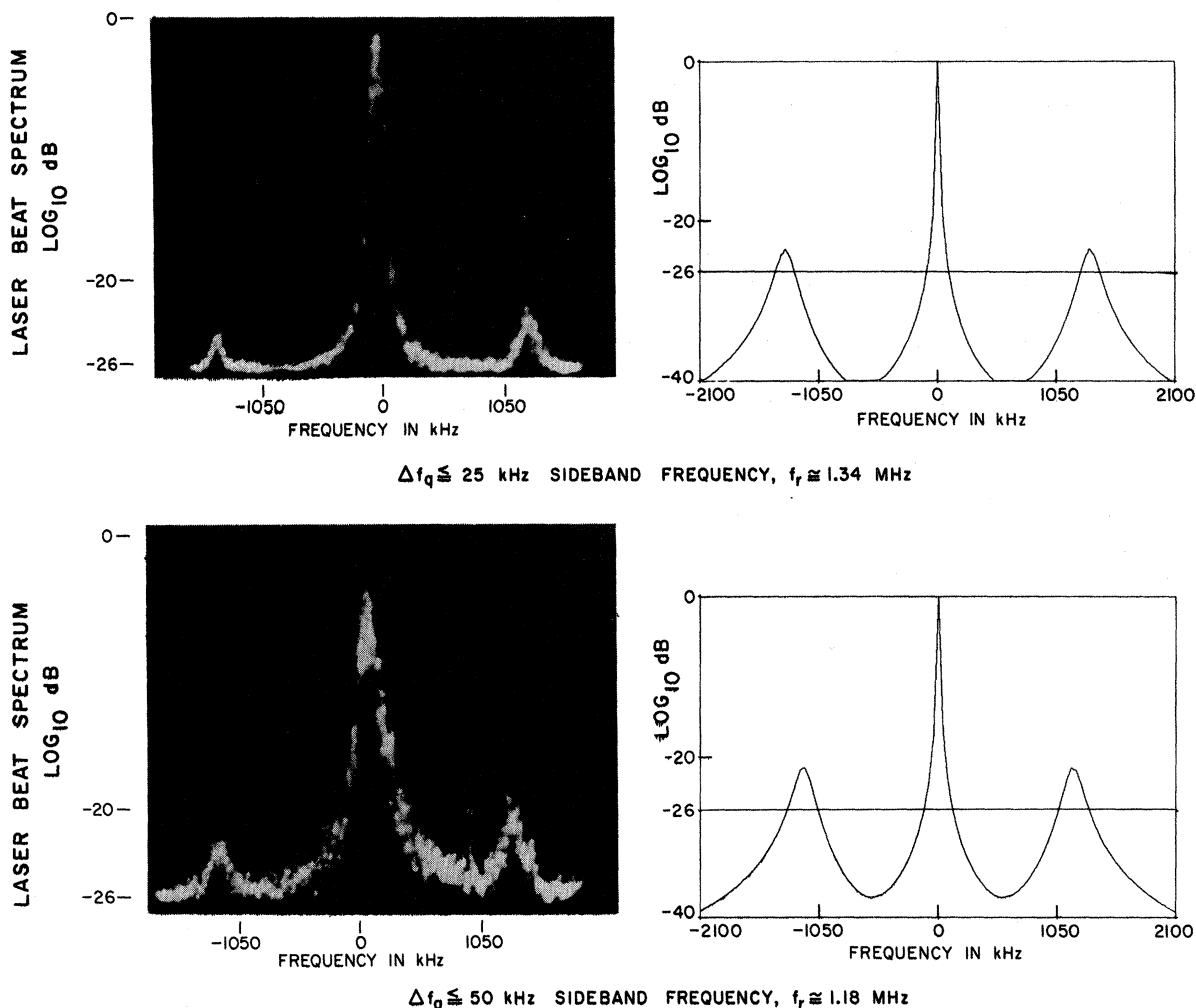


FIG. 10. Power spectrum of the transverse-mode beat at ~ 53 MHz between TEM_{00} and TEM_{01} modes in the He-Xe oscillator. The sidebands on the beat are caused by resonant am modulation or "spiking" in the He-Xe laser system.

laser heterodyne quantum-noise experiment was attempted. The need for frequent refilling of the liquid-nitrogen Dewars, and large backscatter coupling observed between the two lasers, made this experiment unsuccessful. As a simpler experiment, a single laser oscillator followed by a He-Xe laser amplifier was set up as shown in Fig. 9. The xenon pressure and the mode-control irises in the laser oscillator were adjusted until a scanning Fabry-Perot showed that the laser oscillator was supporting only two modes. The mode patterns and the frequency separation between modes indicated that these were the TEM_{00} and TEM_{01} modes of the oscillator. Photographs of the intermode beat spectra between these two modes were than taken as the TEM_{01} mode was driven to its threshold by tuning this mode close to the edge of the atomic-gain curve. The use of two modes in a single laser to study oscillation

linewidths in this fashion has been previously discussed by others.²⁶ The 20-cm-long He-Xe laser amplifier was used as a preamplifier between the laser oscillator and the detector. This laser amplifier had a measured small-signal gain of 130 dB/m, and its use substantially improved the signal-to-noise ratio of the detection system. Both the two-mode laser oscillator and the amplifier were driven by the same carefully regulated 20-MHz rf supply. This supply was continuously monitored by one of our spectrum analyzers to ensure that its output, the laser pumping signal, was free of unwanted modulation.

B. Experimental Results

Figure 10 shows representative photographs of the intermode beat spectrum at ~ 53 MHz as the TEM_{01} mode was driven to threshold. Substantially the same spectra resulted whether this was ac-

complished by tuning the cavity length and thus the cavity frequency, or by reducing the pump level. Some broadening of the beat spectrum is apparent, but more striking are the appearance of sidebands. The frequency spacing of these sidebands tuned linearly with the output level of the beat note. The upper-half of Fig. 11 illustrates the method of tuning the TEM_{01} mode to the edge of the atomic-gain profile, while the lower half of Fig. 11 is a plot of the observed sideband frequency spacing versus beat level. We interpret these sidebands as representing amplitude fluctuations in the laser output, caused by a "ringing" or coupled oscillatory behavior of the atomic populations and the oscillation signal level in the laser cavity. As such, these sidebands are essentially identical to the amplitude-ringing and "spiking" effects more commonly seen in solid-state lasers. The time constants of the He-Xe system are such that this type of behavior is theoretically expected.

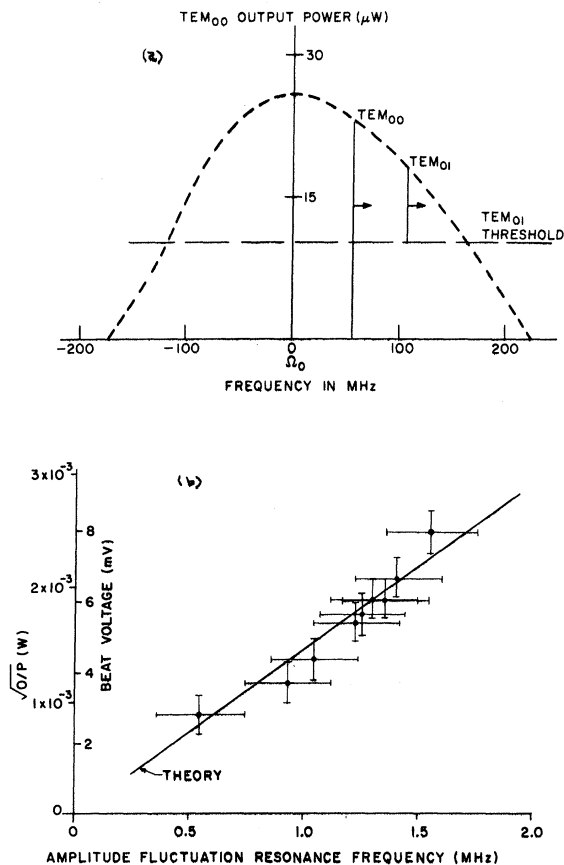


FIG. 11 (a) Illustrating how the TEM_{01} mode can be brought arbitrarily close to threshold by piezoelectrically tuning both the TEM_{00} and TEM_{01} modes across the atomic linewidth. (b) Resonance frequency of the am sidebands in Fig. 10 as a function of the TEM_{01} power level. The theoretical curve is fitted to the data at one point.

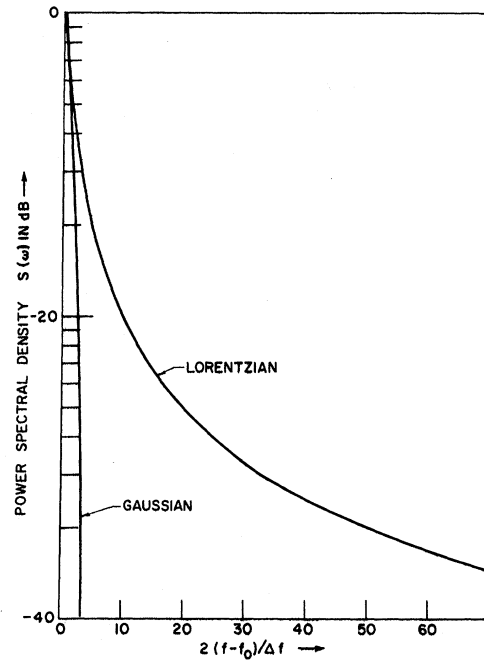


FIG. 12. Comparison of Gaussian and Lorentzian power spectral densities with the same half-width when plotted on a log intensity scale.

The TEM_{01} mode power could not be measured independently of the TEM_{00} mode power in these experiments. The TEM_{00} mode power also changed with frequency tuning, so that it did not provide a constant-amplitude local oscillator, and a correction was required. Intermode frequency pulling effects between these modes were also clearly observed in our experiments, indicating that the two modes were not entirely independent oscillators. For these reasons the above data constitute only a qualitative check of the laser theory. The general behavior of the amplitude-fluctuation sidebands was, however, as predicted by theory, i.e., the sidebands became more prominent and moved closer to the center beat frequency as the TEM_{01} mode approached its threshold.

V. GAUSSIAN SPECTRAL BROADENING AND BACKSCATTERING EFFECTS

The measurements of the quantum-noise linewidth Δf_q reported above were made in the presence of Gaussian spectral broadening of the lasers due to a variety of technical-noise sources. The true laser spectrum is, therefore, more accurately represented as the convolution of the Lorentzian quantum-noise spectrum with a Gaussian frequency-fluctuation spectrum having a bandwidth, in our case, of a few kHz. Figure 12 is a computed plot of Gaussian and Lorentzian power spectral densities having the same linewidth at half-maximum as

they would be displayed by a spectrum analyzer on the \log_{10} setting. The Gaussian linewidth must be more than ten times the Lorentzian linewidth before the Gaussian can mask the wings of the Lorentzian in such a display. Nonetheless, the Gaussian technical-noise contributions will dominate in practical experiments unless particular care is taken to reduce these contributions. Thus, in order to reduce the Gaussian linewidth contribution below 1 kHz in our experiments, all technical-noise sources had to be reduced until the effective rms motions of the laser mirrors were less than 0.03 Å in our 30-cm-long lasers. With sufficiently rigid structures, vibration isolation, sealed intracavity air paths, and a quiet plasma, this stringent requirement could be met.

A. Backscatter Laser Coupling Effects

The low reflectivity of its output mirror makes the signal laser in our experiments particularly susceptible to backscattered radiation from other optical elements. Backscatter of its own output radiation into a laser causes frequency instability, especially if the backscattering elements move and thus change the phase of the backscattered radiation. An even more serious problem is backscattered radiation from the much stronger local-oscillator laser into the signal laser. This backscattered radiation causes frequency pulling and injection-locking effects in the signal laser. The signal laser is particularly susceptible to injection-locking effects at the smaller beat frequencies employed in these heterodyne experiments.

Figure 13 is a schematic showing the principle optical elements relevant to a backscatter analysis of the 3.39- μ two-laser system. Here r and t are complex voltage reflection and transmission coefficients subscripted to identify the optical component. For weak backscattering, the local-oscillator radiation scattered back from the detector into the signal-laser cavity is given by

$$t_{LO} t_S r_{BS} t_{BS} t_p^2 r_d a_{LO} \equiv \gamma e^{i\theta} a_{LO}, \quad (8)$$

where a_{LO} is the oscillation amplitude inside the local-oscillator laser. The various r and t coefficients are defined as in Fig. 13, and γ and θ summarize the amplitude and phase of the net backscatter coefficient. A first-order estimate of backscattering effects in the signal laser is then obtained by substituting $[a + \gamma e^{i\omega_B t + i\theta} a_{LO}]$ for the signal-laser amplitude a in the laser analysis.¹⁵ From this it can be found that the amplitude of the signal-laser oscillation a is affected very little by the backscattered radiation. However, the phase $\varphi(t)$ of the signal-laser oscillation becomes modulated according to the Adler equation²⁷

$$\dot{\varphi}(t) = \omega_L \sin[\omega_B t + \varphi(t) - \theta], \quad (9)$$

where $\omega_L = a_{LO}\gamma/2a\tau_c$ is the locking frequency, i.e., the minimum beat frequency between the two lasers below which the backscattered local-oscillator radiation will injection-lock the signal laser.

The solution to the Adler equation given by Johnson²⁸ is

$$\omega_B t + \varphi(t) - \theta = \sin^{-1} \left(\frac{(\omega_B/\omega_L) \sin(\beta + \delta) - 1}{(\omega_B/\omega_L) - \sin(\beta + \delta)} \right), \quad (10)$$

where $\beta = (\omega_B^2 - \omega_L^2)^{1/2} (t - t_0)$, $\sin\delta = -\omega_L/\omega_B$, and t_0 is chosen so that $\omega_B t_0 + \varphi(t_0) = \theta$. As ω_B approaches ω_L from outside the locking range, the beat waveform should distort dramatically from a sine wave just before the signal laser jumps into lock and the beat note disappears entirely. The shape of the beat waveform depends on the relative phase θ of the backscattered signal, and this depends in turn on the total optical distance from the output mirror of the local-oscillator laser through the backscattering path to the output mirror of the signal laser.

In practice the phase angle θ can be seen to vary through one cycle or one infrared wavelength in a few tenths of a second, due to changes in the total backscatter path, which is some 6 m long. Figure 14 is a single-trace photograph showing the beat between the two 3.39- μ lasers going into lock at a locking frequency $\omega_L/2\pi \approx 9$ kHz. This photograph was obtained by servolocking the lasers at a low beat frequency, and then lowering the discriminator center frequency until locking was observed. The distorted beat waveform just before locking occurs is in excellent agreement with the "cosine" waveform predicted by Eq. (10) as illustrated by the calculated waveform in the lower part of Fig. 14. From the known power levels of the two laser oscillators and the known transmission and reflection coefficients of the laser mirrors and beam splitter, we can deduce that the observed locking behavior can be accounted for by a backscattering from the detector surface as small as

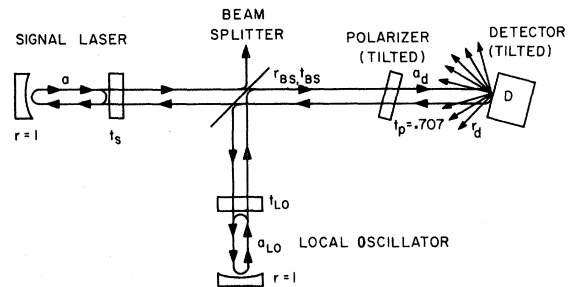
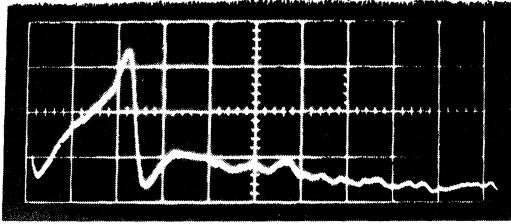
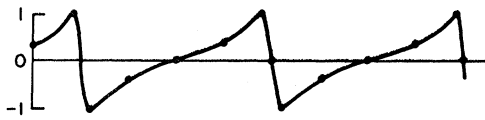


FIG. 13. Schematic of the significant optical elements to be included in an analysis of the backscatter sensitivity of the two-laser heterodyne experiments.



BEAT GOING INTO LOCK AT $\omega_L / 2\pi \sim 9$ kHz
(WAVEFORM FREQUENCY IS ~ 5 kHz)



$\cos[\omega_B t + \phi(t) - \theta_2]$ WAVEFORM, $\frac{\omega_B}{\omega_2} \cong 1.10$

FIG. 14. Experimental observation of the two lasers going into lock as the beat frequency between the lasers approaches the locking frequency; and a theoretical prediction from Adler's equation of the distorted beat waveform to be expected just on the edge of the locking range. The beat goes into a fully locked condition at ~ 3 divisions from the left-hand edge of the oscilloscope tracing.

$|r_d| \leq 1.5 \times 10^{-4}$. The corresponding power reflectivity is -77 dB.

Backscattering of the signal-laser's output into itself can also occur, causing frequency pulling and frequency jitter in the signal laser. The backscattered signal amplitude due to this effect is given by $t_{BS}^2 t_p^2 r_d a = \gamma' e^{i\theta'} a$, and the resulting phase jitter in the signal laser is given by

$$\Delta\varphi(t) = \varphi(t) - \varphi_0 = -[(\gamma'/2\tau_c) \sin\theta'] t, \quad (11)$$

where φ_0 is the initial value of $\varphi(t)$, and τ_c is the signal cavity lifetime. The phase θ' changes randomly with time owing to random changes in the backscatter path length. Assuming that θ' is uniformly distributed in $[0, 2\pi]$ and calculating the mean square change in $\varphi(t)$ over many intervals of length τ leads to

$$[\Delta\varphi^2(\tau)]_{av} = (\gamma'^2/8\tau_c^2) \tau^2 \approx (5.5 \times 10^8) \tau^2. \quad (12)$$

The numerical value is obtained by using the experimental backscatter amplitude deduced from the locking result of Fig. 14.

But, a mean square phase jitter $[\Delta\varphi^2]_{av}$ that increases quadratically with τ implies a Gaussian line broadening for the oscillation with a standard deviation in frequency σ_f given by $(2\pi\sigma_f)^2 = \gamma'^2/8\tau_c^2$, and a full oscillation linewidth given by $(8 \ln 2)^{1/2} \sigma_f$.

Consequently, from our detector backscattering alone, as measured by the locking data above, we may expect a Gaussian line-broadening contribution with a linewidth of approximately 9 kHz for our low- Q signal laser. Experimentally, the Gaussian linewidth was found to be 3 to 5 kHz under the quietest conditions. Some narrowing of the spectrum could be attributed to the AFC loop, but in view of the approximate nature of the calculations and the variable nature of the backscattering and the room disturbances, the agreement is remarkable.

While searching for the dominant backscattering contributions, we locked the lasers at a convenient beat frequency and gently tapped the various optical components while observing the beat frequency. The beam splitter was found to be relatively insensitive, but any disturbances of the detector, indeed, produced a large response. In early experiments, rapidly damped sinusoidal transients appeared intermittently in the instantaneous beat frequency. It was found that these transients corresponded to the barely audible bursting of nitrogen bubbles in the liquid-nitrogen Dewar of the cooled detector. Loosely packing the Dewar with cotton to reduce the bubble size caused these signals to disappear. Other isolation techniques to reduce backscattering were also tried; but, in general, any additional optical elements added to reduce the detector backscattering would themselves give rise to even more serious backscattering problems. The serious difficulties caused by backscattering, both as a source of technical

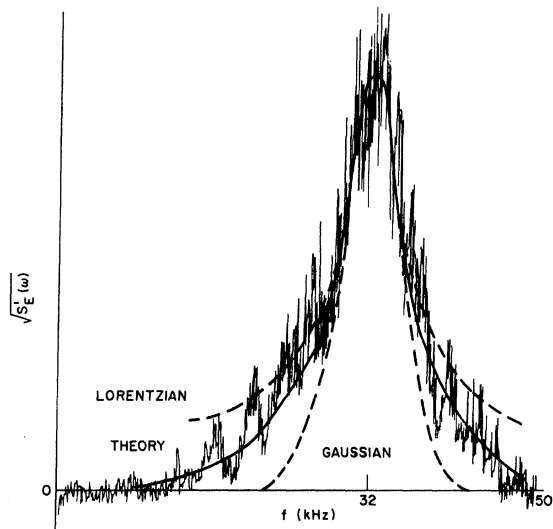


FIG. 15. A representative example of the long-term laser beat spectrum at ~ 32 kHz between the two He-Ne $3.39\text{-}\mu$ lasers, fitted with a theoretical convolution of Gaussian technical-noise and Lorentzian quantum-noise line-broadening contributions.

TABLE I. List of relaxation times.

Medium	Wave-length	Longitudinal relaxation time T_1 (sec)	Transverse relaxation time T_2 (sec)	Doppler linewidth (MHz)
He-Ne	3.39 μ	$\sim 2 \times 10^{-8}$	1.28×10^{-9}	315
He-Ne	6328 \AA	2×10^{-8}	1.59×10^{-9}	1300
He-Xe	3.508 μ	$\sim 1 \times 10^{-6}$	$\sim 4.5 \times 10^8$	~ 107

noise in the signal-laser spectrum and as a source of coupling between the signal and local-oscillator lasers, is clearly indicated.

B. Long-Term Laser Spectrum

In order to investigate the long-term laser spectral width in more detail, the two 3.39- μ lasers were locked at a beat frequency of ~ 32 kHz. The beat spectrum was then scanned and recorded in ~ 2 min using the Hewlett-Packard 302A wave analyzer. Figure 15 is one such recording. The observed spectrum is neither purely Lorentzian nor purely Gaussian and is best fitted by a convolution of the two. The theoretical curve in Fig. 15 was obtained using a Gaussian linewidth contribution of 4 kHz together with a Lorentzian quantum-noise linewidth contribution of 1.5 kHz.

VI. DISCUSSION

A. Relaxation Times and Excess-Noise Factor

Table I lists the relaxation times used in this study. The He-Ne data are available in the literature,^{29, 30} and the He-Xe data are taken from recent work in our laboratory.³¹

In calculating the theoretical linewidths for Figs. 3, 5, and 7, a value must be assigned to the excess-noise factor. We have used the value

$$N_2^c / \Delta N_0 \approx N_2 / (N_2 - N_1) \approx 1.56, \quad (13)$$

as determined by spectroscopic methods for a He-Ne 3.39- μ amplifier by Paananen and co-workers.³² The unsaturated gain coefficient in their experiments was very close to the value required to reach threshold in our lowest- Q laser, so that the level populations in our lowest- Q laser oscillator may not be greatly different from their results.

One might expect that the excess-noise factor should increase with pump current or with laser output power in a given laser, since the upper-level population will increase with increasing current, while the population difference must always stay constant at just the threshold value. A very

rough estimate indicates that the excess-noise factor in our experimental situation might increase from a threshold value of 1.56 to ~ 2.0 at the maximum power level. This would give a deviation from a strict inverse power dependence in the Schawlow-Townes formula. Such a deviation is suggested by the experimental data in Fig. 7, but it is not possible to confirm this within the experimental error of the measurements.

For the He-Xe 3.508- μ laser a value of 1.6 for the excess-noise factor has been reported by Klüber.³³

B. Possible Extention of Measurements through Threshold

The signal-to-noise ratio for optical heterodyne detection may be written as

$$S/N = 2P_{LO} P_S [D^*(\lambda)]^2 / AB, \quad (14)$$

where P_{LO} and P_S are the local-oscillator and signal power levels, respectively, A is the effective area of the detector, B is the bandwidth of the detection system, and $D^*(\lambda)$ is the detectivity of the detector. Given typical values of $D^*(\lambda)$ for our detectors,³⁴ we calculate that we should be able to maintain a 20-dB signal-to-noise ratio for signal powers as low as 10^{-8} – 10^{-9} W. At these low powers the signal laser would be below threshold, and one might be able to observe the predicted factor of 2 increase in laser spectral width as the oscillator passes from above threshold to below threshold. However, our present AFC systems generally fail to maintain locking below signal powers of $\sim 10^{-6}$ W. This occurs because of backscatter coupling and injection-locking between the local-oscillator and signal lasers when lower beat frequencies (below 500 kHz) are employed. For higher beat frequencies where injection-locking would be less serious we have used a room-temperature InAs detector followed by a narrow-band (250 kHz) amplifier. The detectivity of the InAs detector is not good enough, and the amplifier bandwidth is too narrow to pass the entire beat spectrum at lower laser power levels. With a sufficiently sensitive detector operable at a beat frequency of at least several MHz if not higher, and a sufficiently wide amplifier bandwidth, one could hope to maintain frequency lock and to measure the signal-laser spectral width at much lower output power levels, including through the threshold region.

ACKNOWLEDGMENTS

We appreciate the contributions to this work of Dr. S. C. Wang and Professor S. E. Harris, Professor R. L. Byer, and Professor W. Streifer.

*Work supported by the Joint Services Electronics Program at Stanford University, and by the National Aeronautics and Space Administration under NASA Grant No. NGL-05-020-103.

†Present address: Department of Electrical Engineering, University of Alberta, Edmonton, Canada.

¹Yu. N. Zaitsev and D. P. Stepanov, Zh. Eksperim. i Teor. Fiz. Pis'ma v Redaktsiyu **6**, (1967) [Sov. Phys. JETP Letters **6**, 209 (1967)].

²C. Freed and H. A. Haus, Phys. Rev. **141**, 287 (1966).

³J. A. Armstrong, in *Progress in Optics*, edited by E. Wolf (Wiley, New York, 1967), Vol. VI.

⁴F. T. Arecchi, in *E. Fermi Summer School, XLII Convocation on Quantum Optics*, Varenna, Italy, 1967 (Academic, New York, 1968).

⁵I. A. Andronova, Zh. Eksperim. i Teor. Fiz. **56**, 417 (1969) [Sov. Phys. JETP **29**, 227 (1969)].

⁶D. E. McCumber, Phys. Rev. **141**, 306 (1966).

⁷A. E. Siegman and R. Arrathoon, Phys. Rev. Letters **20**, 901 (1968).

⁸R. Arrathoon and A. E. Siegman, J. Appl. Phys. **40**, 910 (1969).

⁹Yu. I. Zaitsev and D. P. Stepanov, Zh. Eksperim. i Teor. Fiz. **55**, 1645 (1968) [Sov. Phys. JETP **28**, 863 (1969)].

¹⁰E. D. Hinkley and C. Freed, Phys. Rev. Letters **23**, 177 (1969).

¹¹M. Lax, in *Physics of Quantum Electronics*, edited by P. L. Kelley, B. Lax, and P. E. Tannenwald (McGraw-Hill, New York, 1966), p. 735.

¹²A. L. Schawlow and C. H. Townes, Phys. Rev. **112**, 1940 (1958).

¹³J. A. Armstrong and A. W. Smith, Appl. Phys. Letters **4**, 196 (1964).

¹⁴A. E. Siegman, B. Daino, and K. R. Manes, IEEE J. Quantum Electron. **QE-3**, 180 (1967).

¹⁵K. R. Manes, Ph. D. dissertation (Stanford University, 1970) (unpublished).

¹⁶W. Louisell, *Radiation and Noise in Quantum Elec-*

tronics (McGraw-Hill, New York, 1964).

¹⁷R. H. Pantell and H. E. Puthoff, *Fundamentals of Quantum Electronics* (Wiley, New York, 1969).

¹⁸M. Lax, *Fluctuation and Coherence Phenomena in Classical and Quantum Physics*, Brandeis University Summer Institute of Theoretical Physics, 1966 (unpublished).

¹⁹A. E. Siegman, *An Introduction to Masers and Lasers* (McGraw-Hill, New York, 1971).

²⁰A. Yariv, *Quantum Electronics* (Wiley, New York, 1967).

²¹B. D. Fried and Samuel D. Conte, *The Plasma Dispersion Function* (Academic, New York, 1961).

²²H. Haken, in *Dynamical Processes in Solid State Optics*, edited by R. Kubo and H. Kamimura (Benjamin, New York, 1967).

²³M. Lax, in *Dynamical Processes in Solid State Optics*, edited by R. Kubo and H. Kamimura (Benjamin, New York, 1967).

²⁴R. A. Paananen and D. L. Bobroff, Appl. Phys. Letters **2**, 99 (1963).

²⁵J. A. Collinson, Bell System Tech. J. **1511** (1965).

²⁶Yu. P. Egorov, Zh. Eksperim. i Teor. Fiz. Pis'ma v Redaktsiyu **8**, 525 (1968) [Sov. Phys. JETP Letters **8**, 320 (1968)].

²⁷R. Adler, Proc. IRE **34**, 351 (1946).

²⁸J. R. Johnson, IEEE J. Quantum Electron. **QE-5**, 7 (1969).

²⁹G. A. Massey, Stanford University Microwave Laboratory Report No. 1812, 1969 (unpublished).

³⁰P. W. Smith, J. Appl. Phys. **37**, 2089 (1966).

³¹S. C. Wang, R. L. Byer, and A. E. Siegman, Appl. Phys. Letters **17**, 120 (1970).

³²R. A. Paananen, H. Statz, D. L. Bobroff, and H. Adams, Jr., Appl. Phys. Letters **4**, 149 (1964).

³³J. W. Kluver, J. Appl. Phys. **37**, 2987 (1966).

³⁴H. G. Heard, *Laser Parameter Measurements Handbook* (Wiley, New York, 1968).

Boundary Energy of a Bose Gas in One Dimension*

M. Gaudin†

Institute for Theoretical Physics, State University of New York, Stony Brook, New York 11790

(Received 25 February 1971)

By the superposition of Bethe's wave functions, using the Lieb's solution for the system of identical bosons interacting in one dimension via a δ -function potential, we construct the wave function of the corresponding system enclosed in a box by imposing the boundary condition that the wave function must vanish at the two ends of an interval. Coupled equations for the energy levels are derived, and approximately solved in the thermodynamic limit in order to calculate the boundary energy of this Bose gas in its ground state. The method of superposition is also applied to the analogous problem of the Heisenberg-Ising chain (not the ring).

I. INTRODUCTION

Let us consider the system of N identical bosons in one dimension interacting via a two-body δ -function potential of strength $2c$. In the repulsive case

$c > 0$, the extensive properties are obtained by enclosing the system in a finite region of space. In one dimension, the simplest way of enclosing the system is to put the N particles on a circle of length L , avoiding boundary considerations, which

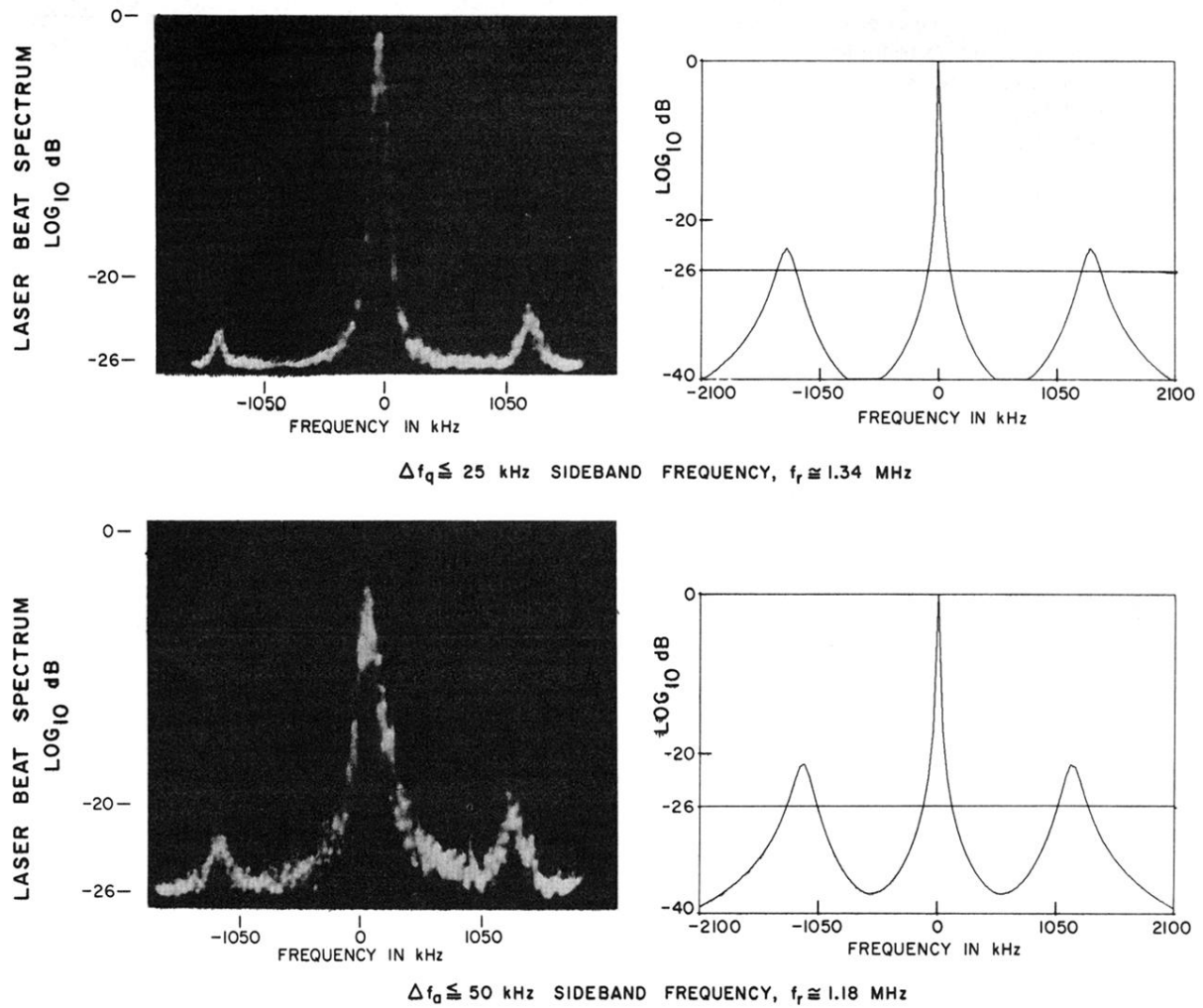
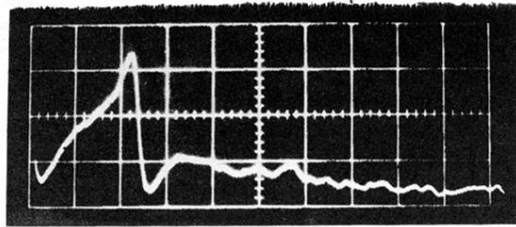
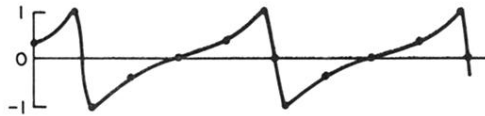


FIG. 10. Power spectrum of the transverse-mode beat at $\sim 53 \text{ MHz}$ between TEM_{00} and TEM_{01} modes in the He-Xe oscillator. The sidebands on the beat are caused by resonant am modulation or "spiking" in the He-Xe laser system.



BEAT GOING INTO LOCK AT $\omega_L / 2\pi \sim 9$ kHz
(WAVEFORM FREQUENCY IS ~ 5 kHz)



$\cos[\omega_B t + \phi(t) - \theta_2]$ WAVEFORM, $\frac{\omega_B}{\omega_2} \cong 1.10$

FIG. 14. Experimental observation of the two lasers going into lock as the beat frequency between the lasers approaches the locking frequency; and a theoretical prediction from Adler's equation of the distorted beat waveform to be expected just on the edge of the locking range. The beat goes into a fully locked condition at ~ 3 divisions from the left-hand edge of the oscilloscope tracing.

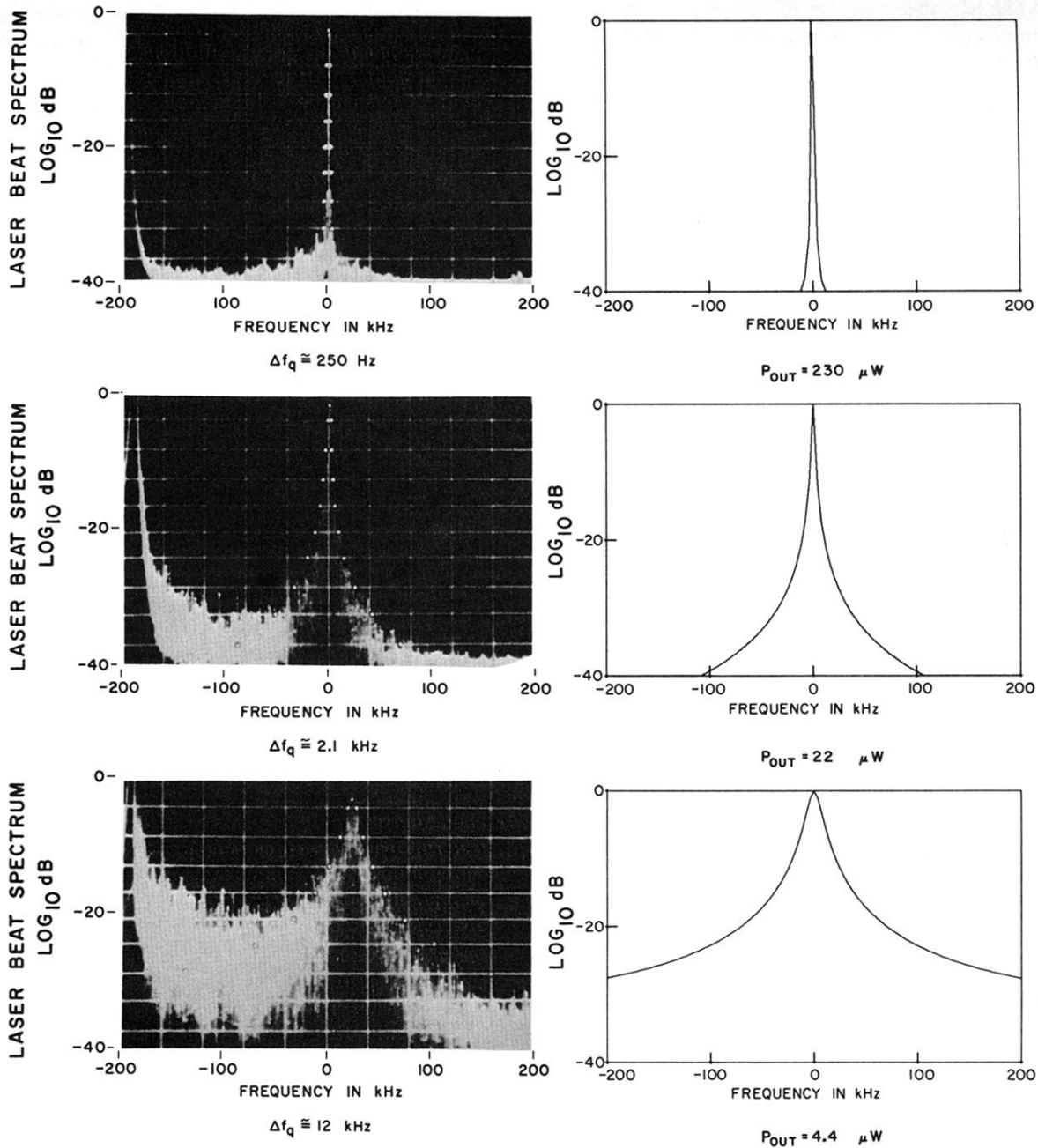


FIG. 2. Power spectrum (on log scale) on the 190-kHz beat between two He-Ne $3.39\text{-}\mu$ lasers at three different output power levels of the signal laser, compared with computer-calculated curves. Laser output mirror reflectivity $\approx 3.5\%$, laser tuned to atomic line center.

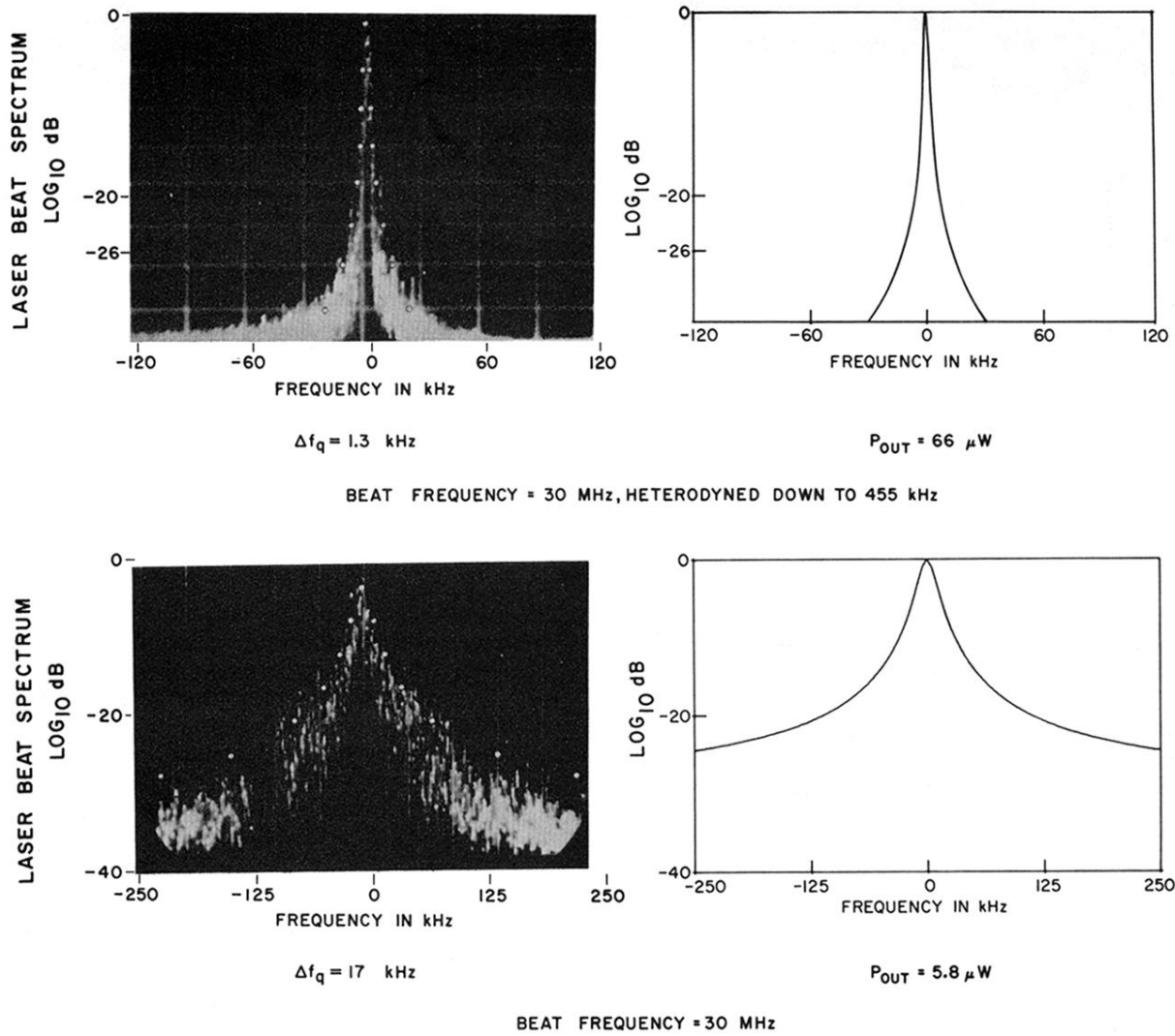


FIG. 6. Power spectrum of the 30-MHz beat between two He-Ne 3.39- μ lasers, on log scale, and corresponding theoretical curves, with the lasers tuned off line center. Output mirror reflectivity $\approx 3.5\%$; signal laser tuned ~ 220 MHz off line center.